UCRL-92371
PREPRINT

DESIGN OF AGGRESSIVE SUPERCONDUCTING TFCX MAGNET SYSTEMS

J. R. Miller

CIRCULATION COPY
SUBJECT TO RECALL
IN TWO WEEKS

This paper was prepared for submittal to the
6th Topical Meeting on the Technology of Fusion Energy,
San Francisco, California, March 3-7, 1985

March 29, 1985

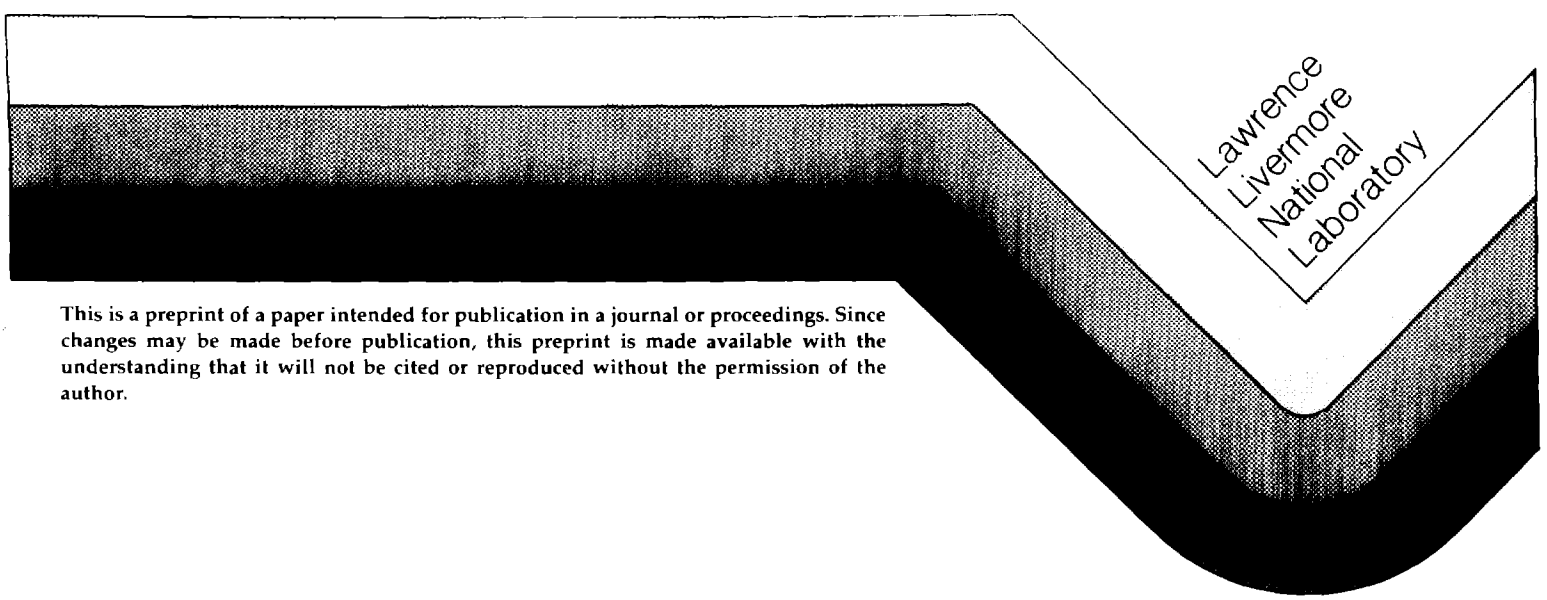

This is a preprint of a paper intended for publication in a journal or proceedings. Since changes may be made before publication, this preprint is made available with the understanding that it will not be cited or reproduced without the permission of the author.

DISCLAIMER

This document was prepared as an account of work sponsored by an agency of the United States Government. Neither the United States Government nor the University of California nor any of their employees, makes any warranty, express or implied, or assumes any legal liability or responsibility for the accuracy, completeness, or usefulness of any information, apparatus, product, or process disclosed, or represents that its use would not infringe privately owned rights. Reference herein to any specific commercial products, process, or service by trade name, trademark, manufacturer, or otherwise, does not necessarily constitute or imply its endorsement, recommendation, or favoring by the United States Government or the University of California. The views and opinions of authors expressed herein do not necessarily state or reflect those of the United States Government thereof, and shall not be used for advertising or product endorsement purposes.

DESIGN OF AGGRESSIVE SUPERCONDUCTING TFCX MAGNET SYSTEMS

JOHN R. MILLER
Lawrence Livermore National Laboratory, University of California
Livermore, California 94550
(415) 422-9745

ABSTRACT

An investigation of several fundamental limits of machine design indicate that a machine fitting the specifications of the Tokamak Fusion Core Experiment (TFCX) can be built with both a superconducting toroidal field (TF) coil set and a plasma major radius of less than 3.2 m. This small size is achieved by accepting a peak nuclear heat load of 50 $kW \cdot m^{-3}$ in the TF coil inner leg while operating at a 10-T maximum field with a current density of 35 $A \cdot mm^{-2}$ in the winding pack. This performance, high by traditional standards, is justified based on developments in forced flow conductor technology using Nb_3Sn composite superconductors.

INTRODUCTION

The Tokamak Fusion Core Experiment (TFCX) is a proposed fusion machine with the mission of demonstrating control of a burning DT plasma of elongated cross section for times as long as several hundred seconds. The necessity of safely handling tritium and ensuring that the various components exhibit acceptable performance in a radiation environment presents a formidable challenge, but perhaps a more severe test is designing a machine that gives the desired performance at an acceptable cost in the present austere budget climate.

Often the design of new devices is based heavily on past developments, which is a safe approach, but sometimes inhibits the attainment of goals that are not otherwise precluded by fundamental constraints. This study, for the most part, ignores the historical achievements of specific superconducting magnet projects and examines fundamental developments in superconducting magnet technology to obtain a fresh perspective on the design limits of a major component of a tokamak reactor, the toroidal field (TF) coil system.

*Work performed under the auspices of the U.S. Department of Energy by the Lawrence Livermore National Laboratory under contract number W-7405-ENG-48.

Costs can usually be reduced by minimizing machine size within the constraints of desired performance; but, in this case, a major obstacle to miniaturization is the amount of shielding required inside the toroidal field coils to maintain the radiation heating and damage at acceptable levels. In addition, size and weight may be minimized in the TF coils themselves, but the required level of high-current-density operation is limited by considerations of safety and reliability. In the present exercise, we examine the extent to which winding-pack current density can be reasonably increased and shielding decreased in the quest for a more compact and hopefully cheaper superconducting machine.

CHOICE OF MACHINE PARAMETERS

We avoid questions of plasma physics by restricting our considerations to those already included in the specifications and formulae for engineering variables found in the TFCX Preconceptual Design Specifications.[1] From these formulae, assuming an ignition margin of 1.5, a plasma elongation of 1.6, and a plasma edge safety factor of 2.4, the following relations can be extracted for parameters critical to the design of the TFCX TF magnet system (see list of symbols for definitions):

$$B_{max} = \left(\frac{26.614}{R_p + 1.2763\ a}\right)^{1/3}\left(\frac{R_p^2}{a^{4/3}}\right) \times [R_p - (a + \delta)]^{-1}.$$

$$P_{wall} = 1.3419(R_p + 1.2763\ a)^{-4/3} \times \left(\frac{R_p^2}{a^{2/3}}\right).$$

$$\Delta\phi = 1.68\ a^{2/3}\ (4.152\ R_p + 5.2994\ a)^{2/3} \times \left[1.255 - \frac{(R_p - 4.824\ a)^2}{45.0\ a^2}\right].$$

Except for the appearance of δ in the equation for B_{max}, all terms are functions of R_p and a only. These relationships were chosen for scrutiny because they produce results relating directly to the limitations in achieving compactness in a tokamak with TFCX specifications. Specific contours of each variable are plotted in the a,R_p plane in Fig. 1 with δ = 0.58 m. When δ = 0.58 m there is room, along with other essential components, for 0.31 m of shielding material. If, in addition, the shield is a high-performance shield using tungsten,[2] this 0.31-m thickness translates to a peak nuclear heat load in the TF coil of 50 kW•m^{-3} for a wall loading of 1 MW•m^{-2}. A goal of this study is to demonstrate that a safe, reliable, and compact TF coil design can be conceived to operate with peak heat loads of this magnitude.

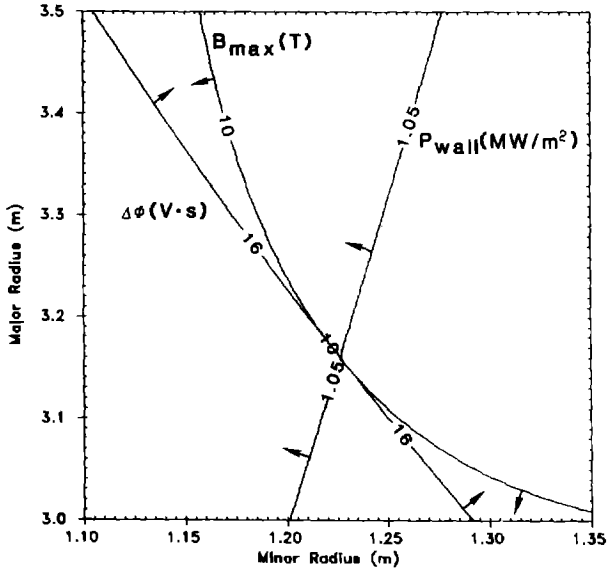

Fig. 1. Contours of maximum magnetic field, neutron wall loading, and required OH flux swing used to size the TF magnet system. Separation (δ = 0.58 m assumed) between inboard edge of plasma and TF winding.

The arrows on contours in Fig. 1 indicate the direction of increasing magnitude of the contoured variable. A particular machine configuration is indicated by the intersection of the three contours. Is it the optimum choice? Probably it is not absolutely, but let us examine the penalties in trying to move away from this point toward a smaller machine, i.e., toward smaller R_p.

Decreasing R_p from the above point decreases the wall loading. This decrease is not rapid and it is not a severe consequence, but there is a desire to keep P_{wall} near 1 MW•m^{-2} to enhance the reactor relevance of the machine. In addition, the flux swing required from the ohmic heating (OH) system decreases. Both of these reductions, however, come at the expense of increasing B_{max} on the TF coil windings. The decision to reduce shielding and accept peak heat loads of 50 kW•m^{-3} makes increased fields difficult to tolerate. But, as discussed later, structural considerations and space requirements for OH coils at the center of the machine also discourage further reductions in R_p. Table I contains a list of parameters describing the TF coil system for the machine in Fig. 1. Some of these values result directly from the particular choice of a and R_p in Fig. 1, whereas others are justified by other considerations in the course of this paper. Still others are not critical in the context of this study and are chosen for convenience only. The basis for each choice is indicated in the table footnotes.

GOALS FOR WINDING-PACK CURRENT DENSITY

In several workshops supporting the pre-conceptual design of TFCX, experts in the field of superconducting magnet development were asked how high they thought the winding-pack current density could reasonably be pushed in coils appropriate for TFCX. Their estimates were based on a number of considerations, including the state of the art of superconductor manufacturing technology, structural problems, coil protection requirements, heat removal, extrapolation of historical achievement, faith, and more. As expected, their projection of a reasonable goal for current density in the winding pack decreased as the design maximum field in the winding pack increased. At 10 T, the panel suggested J_{pack} = 35 A•mm^{-2} as a reasonable goal. This study attempts to justify this choice based on several critical considerations.

CONDUCTOR CHOICE AND COOLING SCHEME

As already mentioned, the reduction in size sought for a "superconducting" TFCX will be achieved at the expense of accepting untraditionally high heat loads in the winding pack. There is risk in attempting to do this with bath cooling because of the possibility of vapor locking the cooling channels. Therefore, I choose from the outset to perform this conceptual design using forced flow of helium at supercritical pressures for cooling. A conductor type that incorporates this cooling technique and simultaneously provides a high margin of stability at a high operating current density is the cable-in-conduit conductor. A well-known example of this type of conductor is pictured in Fig. 2, the Westinghouse/Airco LCP conductor.[3] As in the Westinghouse conductor, the cable strands for purposes of this study will be multifilamentary Nb_3Sn/copper composites. The use of Nb_3Sn, by virtue of its high T_c, permits the removal of high heat loads because temperature in the flowing helium can be

Table I. Parametric description of the superconducting TF-coil system for TFCX.

TF system parameters		
R_p	3.16 m	(1)
a	1.225 m	(1)
B_t	4.288 T	(1)
B_{max}	10.0 T	(1)
NI	67.75 MA•turns	(1)
P_{wall}	1.05 MW•m^{-2}	(1)
t_{shield}	0.31 m	(2)
N_{coils}	16	(2)
R_2	1.355 m	(1)
R'_2	1.385 m	(3)
R'_1	0.98 m	(4)
R_1	1.03	(5)
h	3.2 m	(3)
$\langle R_i \rangle$	1.2 m	(3)
$\langle R_o \rangle$	5.5 m	(3)
L	17 m	(3)
E_s	220 MJ/coil	(4)
Winding pack parameters		
J_{pack}	35 A•mm^{-2}	(2)
A_{pack}	0.121 m^2	(5)
N_{turns}	258	(3)
A_{eff}	(21.66 mm)^2	(3)
f'_{steel}	0.25	(3)
f'_{insul}	0.17	(3)
f'_{cond}	0.34	(6)
f'_{He}	0.24	(6)
Conductor parameters		
J	60.3 A•mm^{-2}	(5)
J_{c0}	920 A•mm^{-2}	(7)
T_c	9.95 K	(7)
f_{cond}	0.59	(6)
f_{Cu}	0.60	(6)
I_{op}	16.4 kA	(5)
H	10^6 J•m^{-3}	(6)

Method of parameter choice:
(1) Examination of machine parameter "specifications" to obtain minimum credible size.
(2) Assumption.
(3) Noncritical assumptions consistent with other fixed parameters of this machine and some judgment of what is "typical".
(4) Calculations from other fixed parameters of this machine using approximate formulae in text.
(5) Direct consequence of the choice of other parameters of this machine.
(6) Consequence of conductor optimization.
(7) Typical superconducting material data where compressive prestrain is included.

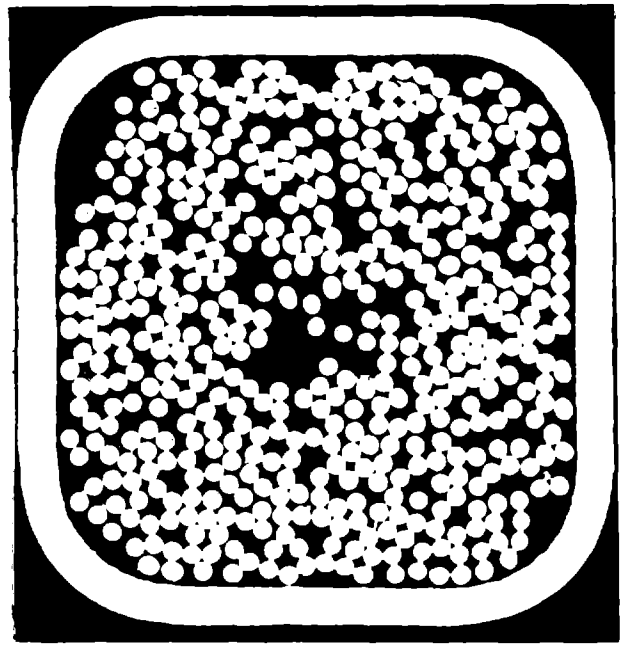

Fig. 2. Cross section of a typical cable-in-conduit superconductor (the Westinghouse/Airco LCP conductor), showing a cable of many Nb_3Sn/copper composite strands contained inside a strong steel sheath that directs the flow of helium at supercritical pressures through the interstices of the cable.

allowed to rise above the usual magnet operating temperature to the 5-to-6-K range, where the heat capacity of the fluid is quite high (especially if the pressure is not much greater than the critical pressure).

Critical current data[4] for strands appropriate to this conductor type are shown in Fig. 3. Below the straight line fit to the data is another line that uses Ekin's method[5] to account for the degradation due to compressive strain on the Nb_3Sn superconductor resulting from differential cooldown strains of the various materials comprising the conductor system. Presently available empirical data on similar conductors indicate that this is the appropriate degradation to expect in a conductor having the composition and void fraction of the cable considered here.[6,7] Use of the degraded temperature-dependent critical-current density in Fig. 3 represents a conservative design approach inasmuch as the design touted here will purposefully permit much of the prestrain to be removed by tension in the windings as the coils are charged to operating field.

STRUCTURAL CONSIDERATIONS

The forces in a tokamak during operation are complex, and it is beyond the scope of this paper to consider them all in detail. However,

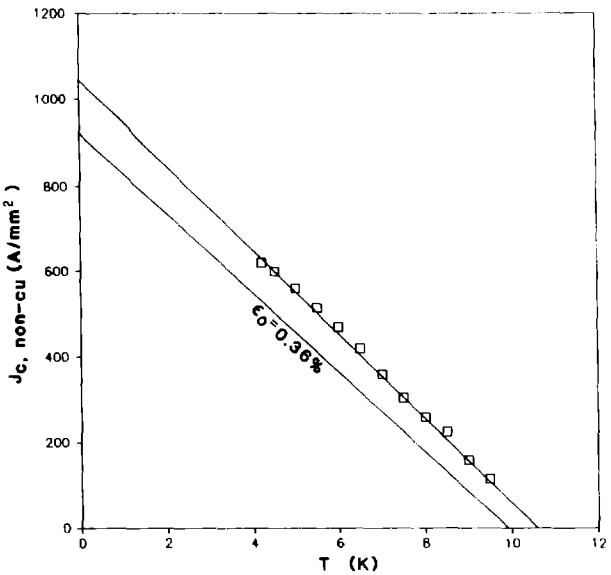

Fig. 3. Critical current data for strands appropriate to a cable-in-conduit superconductor. The line below that fitted to the data includes expected degradation due to compressive strains resulting from cooldown to operating temperature from the Nb_3Sn formation temperature.

the tensile loads and the centering forces on the inner, vertical leg of a TF coil place fundamental lower limits on the cross section of one of these coils. At a minimum, sufficient structural material in the case and winding pack in this critical region must be available to safely support these loads or the design is flawed from the start.

The tension in the inner leg of a TF coil can be expressed as

$$T = \frac{\pi (B_t R_p)^2}{2 N_{coils} \mu_0} \ln\left(\frac{\langle R_o \rangle}{\langle R_i \rangle}\right) .$$

Values for $\langle R_o \rangle$ and $\langle R_i \rangle$ in Table I represent educated but possibly crude guesses that are based on the machine parameters, typical TF coil shapes, and some assumptions about desired shielding thicknesses. However, because they appear in the argument of the natural logarithm, these guesses do not seriously degrade the accuracy of the tension estimate.

The conductor type chosen for this study contains a structurally weak multistrand cable inside a strong steel conduit. In the coil, tensile loads arise from Lorentz forces on the conductor that are subsequently transmitted first to the conduit and then to the case. Therefore, the sheath of the conductor receives at least as much stress as the case, and this should be accounted for in calculating the required support for the tensile loads.

Practical fractions of steel, insulation, conductor, and helium in a winding pack produced from a conductor of the type in Fig. 2 are also found in Table I. The radius R_1' defining the inward extent of a TF coil case is the only variable still available to change the cross section of the TF coil case in the inner leg, and, thereby, affect the tensile stress by changing the amount of structural material. The tensile stress in terms of R_1' and other variables already selected is

$$\sigma_t \approx \frac{T}{\left[\frac{\pi (R_2'^2 - R_1'^2)}{N_{coils}}\right] - (1 - f'_{steel}) A_{pack}} .$$

Choosing the allowable stress as 230 MPa (1/3 the yield value for 304 LN), we find $R_1' = 0.98$ m. If I did not account for the steel in the winding pack, the case would extend into $R_1' = 0.90$ m in order to maintain the same allowable stress limit. With $R_1' = 0.98$ m, $R_1 = 1.03$ m is reasonable for the inward extent of the TF windings. Figure 4 shows a possible configuration of the TF coil case at the midplane of the inner leg using the values of R_1', R_1, R_2, and R_2'. Also indicated are individual turns that are shown with an appropriate, but still somewhat arbitrary, cross section.

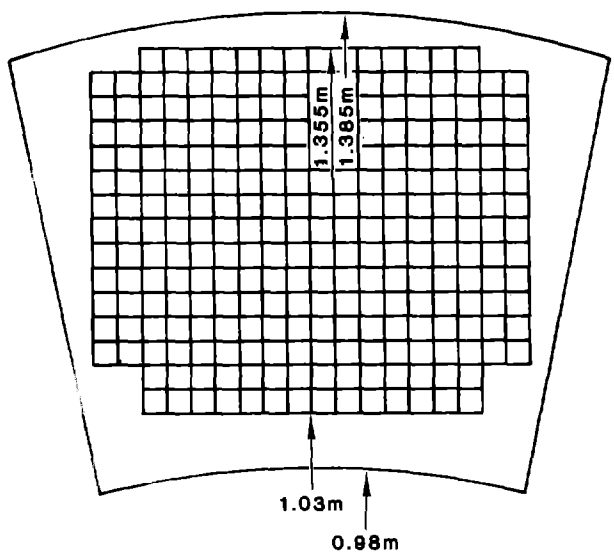

Fig. 4. Cross section of the TF-coil inner leg at the midplane showing the envelope of the case and the winding pack.

By estimating that the total ampere-turns of the TF coils are spread uniformly over the cross section of a cylinder of $R_2 - R_1$ thickness, we derive the following expression for the radial stress at R_1 on the midplane:

$$\sigma_r \approx \frac{B_{max}^2}{2\mu_0}\left[\frac{\frac{8r^2}{3} - 4r + \frac{4}{3r}}{(1 - r^2)^2}\right] ,$$

where $r = R_1/R_2 < 1$. Note that

$$\lim_{r \to 1} \sigma_r = \frac{B_{max}^2}{2\mu_0} ,$$

the limit for thin coils, but for practical cases

$$\sigma_r > \frac{B_{max}^2}{2\mu_0} .$$

In particular, $r = 0.76$ for our case so that $\sigma_r = 56.8$ MPa (8.2 ksi). Note that the above relationships indicate that some small benefit, a reduction in the maximum radial stress, is derived by increasing the current density in the proper manner, i.e., by increasing r toward unity.

SUPERCONDUCTOR STABILITY AND HEAT REMOVAL

The fractions of conductor and helium in the winding pack as listed in Table I are not arbitrary. Rather they represent a choice of conductor parameters to maximize the stability against external perturbations. Following a suggestion by Dresner,[8] the stability margin (per unit volume of conductor) for a conductor of this type that fully uses the heat capacity of the interstitial helium can be cast in the form

$$\Delta H = S_{He}\,(T_{cs} - T_b)(A_{He}/A_{cond}) .$$

The essentially linear variation of critical current density vs temperature apparent in Fig. 3 allows rewriting this expression in the dimensionless form

$$\Delta h = \frac{\Delta H}{S_{He}\,T_c} = \frac{(1 - f_{cond})}{f_{cond}}\left[\left(\frac{T_c - T_b}{T_c}\right) - \frac{J}{f_{cond}\,(1 - f_{Cu})\,J_{co}}\right] .$$

Contours of Δh are plotted in Fig. 5. Also plotted are curves labeled Δh_{max}, representing the locus of optimum f_{cond} for a particular f_{Cu}; $f_{Cu,min}$, representing a choice of the minimum copper fraction in a conductor based on perceived ease of manufacture and the impact on coil protection (discussed later); and J_{lim}, representing a boundary that must not be crossed to ensure that the heat capacity of the interstitial helium is fully used.[9] Safe values of f_{cond} are to the right of J_{lim}. Figure 4 shows that, for the values of the parameters indicated, the optimum choice is $(f_{cond}, f_{Cu}) = (0.59, 0.60)$, which is the intersection of J_{lim} and $f_{Cu,min}$ in this case. Note that this choice is independent of the exact form or value for S_{He}.

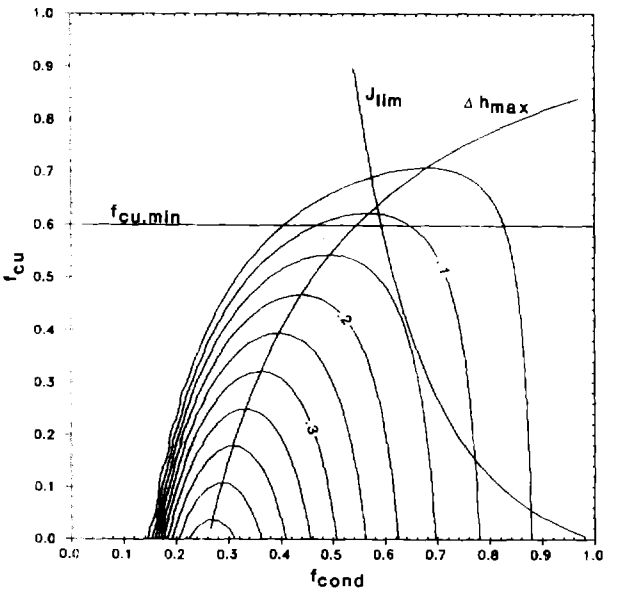

Fig. 5. Contours of dimensionless stability margin used to choose the conductor configuration. Contours were calculated with B = 10 T, T_b = 5.6 K, D_h = 0.6 mm, J_{c0} = 920 A•mm^{-2}, and T_c = 9.95 K. A numerical prefactor of 0.9 has been chosen to calculate J_{lim} from Eq. (1) of Ref. 9 (all variables in SI units).

The choice of T_b = 5.6 K in selecting f_{cond} and f_{Cu} represents foresight in solving the problems of heat removal, recognizing that the temperature in a flow path subjected to nuclear heating will rise relative to the inlet. The inner layer of the TF coil as it passes through the inboard leg represents the most critical region in that it receives the highest heat load while being exposed to the highest field. Some simple considerations will show that a winding scheme can be devised to maintain the temperature of a flow path passing through this region below 5.6 K, and, thereby, provide good conductor stability.

For low enough flow, the temperature rise from inlet to outlet of a heated flow path is inversely proportional to the rate of flow. Eventually, however, frictional effects must dominate causing an increase in the temperature rise with increasing flow. For the case of a noncompressible fluid, a simple, approximate expression for the temperature rise across a flow path can be written as follows:

$$\Delta T \approx L\left[\frac{\langle \dot{q}_n \rangle}{c_p}\left(\frac{1 - f'_{He}}{f'_{He}}\right)\frac{1}{G} + \frac{2f}{c_p \rho_{He}^2 D_h} G^2\right] .$$

The first term will be recognized as the contribution of the external heat and the second, as

the contribution of friction. This relationship has a minimum at

$$G_{opt} \approx \left[\frac{\langle \dot{q}_n \rangle \left(\frac{1 - f'_{He}}{f'_{He}} \right) \rho_{He}^2 D_h}{4f} \right]^{1/3} .$$

In this approximation, the temperature rise for the flow resulting in the minimum is

$$\Delta T \approx 1.5 \, L \left[\frac{4f \langle \dot{q}_n \rangle^2 \left(\frac{1 - f'_{He}}{f'_{He}} \right)^2}{c_p^3 \rho_{He}^2 D_h} \right]^{1/3} .$$

The pressure drop across a flow path resulting from this flow can also be estimated by a simple approximate formula:

$$\Delta p \approx L \left(\frac{2fG^2}{\rho_{He} D_h} \right) .$$

To use these formulae, care must be exercised in choosing the appropriate mean values of the helium properties. In addition, an estimate must be made of the average nuclear heat load along a channel, which requires that some assumptions must be made. On the outboard leg of a TF coil, space is not as precious as near the inboard leg. Assuming that enough shielding can be placed there to reduce the heat load by 1/100; and further assuming that this is achieved in such a way that the variation in heating around a channel in the inner layer of the coil is given by

$$\dot{q}_n(\theta) = \dot{q}_{max} \left[\sin \frac{\theta}{2} + \frac{1}{100} \left(1 - \sin \frac{\theta}{2} \right) \right] ,$$

the average around the circumference must be $\langle \dot{q}_n \rangle = 0.64 \, \dot{q}_{max}$. Detailed studies show this to be a very conservative estimate.[10]

A final assumption must now be made. Assume that each turn of the inside layer can be cooled separately, i.e., helium can be injected at 4.5 K and removed after only one turn resident in the winding. This can be accomplished by penetrating the sheath of the conductor to provide a flow connection without making an electrical joint in the cable inside. Such connections can be made quite simply and can be located anywhere on the outboard leg where space is available. One such connection would be the input point for helium from which flow would divide and send cold helium in opposite directions through adjacent turns. The next connections, one turn away in either direction, would receive warm helium arriving both from that turn and the next adjacent turn, and so on. The technique is similar to one already used successfully in a small solenoid built to demonstrate cable-in-conduit conductor technology[11] except flow connections in that case were between adjacent layers.

Using $\dot{q}_{max} = 50 \text{ kW} \cdot \text{m}^{-3}$ and the appropriate helium properties applied in an iterative fashion to the preceding formulae, the mutually consistent values in Table II can be derived for single turns on the inside, most highly heated sections. The requirement will, of course, be less stringent for layers deeper in the coil since they will, because of their location, be exposed both to less heat and lower magnetic field.

Table II. Helium flow requirements.

G_{opt}	=	$195 \text{ kg} \cdot \text{s}^{-1} \cdot \text{m}^{-2}$
(p_i, T_i)	=	(800 kPa, 4.5 K)
(p_o, T_o)	=	(350 kPa, 5.6 K)
The following approximate values have been used in the calculations.		
ρ_{He}	=	$100 \text{ kg} \cdot \text{m}^{-3}$
f'_{He}	=	0.24
D_h	=	0.6 mm
f	=	0.02
c_p	=	$12 \text{ kJ} \cdot \text{kg}^{-1} \cdot \text{K}^{-1}$
L	=	17 m

With the critical current data of Fig. 3, the chosen fractions of winding pack materials, and the very conservative approximation of $S_{He} = 10^6 \text{ J} \cdot \text{m}^{-3} \cdot \text{K}^{-1}$ at 5.6 K, 4 atm, the stability margin should be in excess of $10^6 \text{ J} \cdot \text{m}^{-3}$ ($1 \text{ J} \cdot \text{cm}^{-3}$) in the most critical part of the coil.

REFRIGERATION COSTS

Minimizing the temperature rise in a flow path may or may not be necessary to attain sufficient stability for reliable coil operation. In the above example, choosing flow paths of only one-turn length made extremely large margins available. However, minimizing the temperature rise to obtain high stability margin comes at a price. Again assuming noncompressible flow, calculations indicate that, for the flow producing the minimum temperature rise, the frictional heat contributes to the total heat load an amount that is 50% of the external heat load. Thus the refrigeration requirement, if the temperature rise must be minimized, would also be an additional 50%. This is a general result of the assumption of noncompressible flow, where the difference in inlet and outlet temperature at low flow is

proportional to G^{-1}; and the temperature increase at higher flow is proportional to G^2. A more efficient means of removing the heat, in terms of refrigeration costs, would be to operate at lower pressures that are near the critical pressure, where the specific heat of the fluid is much higher. Large benefits are available in holding down the refrigeration costs while maintaining stability, but detailed studies beyond the scope of this report are required to demonstrate these benefits.

PROTECTION

Two key issues exist in the protection of a coil using a force-cooled, cable-in-conduit conductor--pressure rise and temperature rise in the event of a quench and dump of the coil. Good experimentally verified formulae are available for these key parameters for "worst case" conditions, namely for the maximum temperature and the maximum pressure in the event that an entire flow path is quenched instantaneously.[12,13] The pressure, in this case, can rise no higher than

$$p_{max} = 0.14 \left(\frac{\dot{q}^2 L^3}{8 D_h} \right)^{0.36} ,$$

even if the coil is not dumped. The maximum temperature, allowing for rapid detection and dump at voltage V_D, is given by

$$T_f = T_i + \left(\frac{E_s}{V_D I_{op}} \right) \left(\frac{f^2 \rho_{Cu}}{f_{Cu} f_{cond} (1 - f_{cond}) \rho_{He,i} \langle C_v \rangle} \right) .$$

This calculation represents an extreme estimation of the maximum temperature because it accounts only for the heat capacity of the helium trapped inside the conduit. This calculation does not account for the heat capacity of the conductor nor of the sheath material, both of which contribute significant heat capacity at temperatures $\sim$10 K and greater.

The stored energy per coil of the TF coil set can be approximated by

$$E_s \approx \frac{\pi^2 (B_t R_p)^2 h}{2\mu_0 N_{coils}} \ln \left(\frac{\langle R_o \rangle}{\langle R_i \rangle} \right)$$

to be about 220 MJ. Taking the dump voltage as V_D = 3 kV, a safe value for this type of conductor, yields a conservative estimate of about 200 K for the final temperature in a completely quenched coil. The pressure in the worst case can rise no higher than 3 MPa.

CONCLUSIONS

A machine meeting the TFCX requirements can be designed having a plasma major radius between 3.1 and 3.2 m. To justify this small size, I have demonstrated the feasibility of superconducting TF coils producing 10-T maximum field with a winding-pack current density of 35 $A \cdot mm^{-2}$, while accepting a peak nuclear heat load of 50 $kW \cdot m^{-3}$. The design of these coils is within the current state of the art of superconductor manufacturing technology, the minimum structural requirements, the space requirements for a central OH solenoid, and the protection requirements for the coil set. The least margin available in using this small size is in the area of safely supporting the stresses resulting from the centering forces on the TF coils. Consideration should be given to increasing the goal for winding-pack current density in a manner that would reduce these stresses.

ACKNOWLEDGMENTS

I would like to extend my sincere appreciation to B. G. Logan and C. D. Henning for calling attention to the need for compact fusion magnets and suggesting the approach for obtaining them. I would also like to thank E. N. C. Dalder for his support and encouragement during the course of this study. In addition, much of the technology of force-cooled conductors presented here, some of it heretofore unpublished, was developed in cooperation with J. W. Lue and L. Dresner, and I gratefully acknowledge their contributions.

LIST OF SYMBOLS

a (m)	Plasma minor radius
A_{pack} (m^2)	Cross-sectional area of the winding pack of one TF coil
A_{eff} (m^2)	Effective cross-sectional area of one turn of the winding pack
B_{max} (T)	Maximum magnetic field on the windings of a TF coil
B_t (T)	Magnetic field on the plasma axis
c_p ($J \cdot kg^{-1} \cdot K^{-1}$)	Specific heat at constant pressure of the helium
c_v ($J \cdot kg^{-1} \cdot K^{-1}$)	Specific heat at constant volume of helium
D_h (m)	Hydraulic diameter of the helium cross section of a flow path
D_w (m)	Diameter of a cable strand
E_s (J)	Stored energy per coil of the TF coil set at full field
f	Friction factor for a flow path (taken as approximately constant value of 0.02 for this study)[13]

f_{cond}	Fraction of conductor (including copper and superconductor) inside the conductor sheath
f_{Cu}	Fraction of copper in a conductor strand
f'_{cond}	Fraction of conductor (including copper and superconductor) in the winding pack
f'_{He}	Fraction of helium in the winding pack
f'_{insul}	Fraction of insulation material in the winding pack
f'_{steel}	Fraction of steel (as conduit material) in the winding pack
G ($kg \cdot m^{-2} \cdot s^{-1}$)	Mass flow per unit helium cross section of a flow path
G_{opt} ($kg \cdot m^{-2} \cdot s^{-1}$)	Value of G giving the minimum temperature rise along a flow path
h (m)	Vertical distance from the machine midplane to the midpoint of the TF-coil winding pack
I_{op} (A)	Operating current for a TF coil
J ($A \cdot m^{-2}$)	Current density over the cable space of the conductor, i.e., inside the conduit
J_{c0} ($A \cdot m^{-2}$)	Critical current density at operating magnetic field referred to the non-copper fraction of a strand and extrapolated to 0 K
J_{pack} ($A \cdot m^{-2}$)	Operating current density referred to the winding-pack cross section
L (m)	Length of a flow path (therefore, approximately the mean circumference of a TF coil)
N_{coils}	Number of coils in the TF system
N_{turns}	Number of turns in a single TF coil
NI (A•turns)	Total ampere•turns in the TF-coil system
P_{wall} ($MW \cdot m^{-2}$)	Neutron wall loading on the first wall
p_i (Pa)	Absolute pressure of helium at the inlet of a flow path
p_o (Pa)	Absolute pressure of helium at the outlet of a flow path
p_{max} (Pa)	Maximum absolute pressure in a flow path resulting from "worst case" quench conditions
$\dot{q}_{He}$ ($W \cdot m^{-3}$)	Power density to the helium in a flow path resulting from joule heating in the conductor stabilizer following a quench
$\dot{q}_n$ ($W \cdot m^{-3}$)	Power density to the solid portion of a coil resulting from nuclear absorption
$\dot{q}_{max}$ ($W \cdot m^{-3}$)	Maximum of q_n in the winding pack
r	Ratio of R_1 and R_2
R_p (m)	Radius from the machine axis to the axis of the plasma
R_1 (m)	Radius on the midplane from the machine axis to the centermost turns in the winding pack of a TF-coil inner leg
R_2 (m)	Radius on the midplane from the machine axis to the turns in the winding pack of a TF-coil inner leg nearest the plasma
R'_1 (m)	Radius on the midplane from the machine axis to the centermost portion of the case of a TF-coil inner leg
R'_2 (m)	Radius on the midplane from the machine axis to the portion of the case of a TF-coil inner leg nearest the plasma
$\langle R_i \rangle$ (m)	Mean radius on the midplane from the machine axis to the TF-coil inner leg
$\langle R_o \rangle$ (m)	Mean radius on the midplane from the machine axis to the TF-coil outer leg
S_{He} ($J \cdot m^{-3} \cdot K^{-1}$)	Effective volumetric heat capacity of the interstitial helium in a cable-in-conduit conductor

t_{shield} (m)	Thickness of the nuclear shield between the first wall and the TF-coil inner leg
T_b (K)	Bulk fluid temperature of the helium in a flow path
T_c (K)	Critical temperature of the superconductor at operating magnetic field
T_{cs} (K)	Current sharing temperature of the superconductor at the operating field and current
T_f (K)	Final temperature in the TF coil after a quench and dump of the stored energy
T_i (K)	Initial temperature in a TF coil before a quench or the temperature of the helium at the inlet of a flow path
T_o (K)	Temperature of the helium at the outlet of a flow path
V_D (V)	Voltage across the terminals of a TF coil at the beginning of a dump of the stored energy
δ (m)	Radial distance on the mid-plane between the plasma edge and the near surface of the winding pack in the TF- coil inner leg
Δh	Dimensionless stability margin of the cable-in-conduit conductor against external perturbations
ΔH ($J \cdot m^{-3}$)	Stability margin of the cable-in-conduit conductor against external pertubations
Δp (Pa)	Pressure drop in the helium in a flow path between inlet and outlet
ΔT (K)	Temperature rise in the helium in a flow path between inlet and outlet
$\Delta \phi$ (Wb)	Flux swing required from OH coils during burn
ρ_{Cu} ($\Omega \cdot m$)	Resitivity of the copper stabilizer at operating temperature and magnetic field
ρ_{He} ($kg \cdot m^{-3}$)	Density of the helium at operating temperature and pressure

REFERENCES

1. G. V. SHEFFIELD, TFCX Preconceptual Design Specifications, Rev. 0, TFCX Engineering Office, Princeton Plasma Physics Laboratory, Princeton, NJ (1984).

2. J. D. LEE, Lawrence Livermore National Laboratory, Livermore, CA, private communication (June 1984).

3. J. L. YOUNG, C. J. HEYNE, P. KOMAREK, H. KRAUTH, G. VECSAY, and C. MARINUCCI, in Advances in Cryogenic Engineering, (Plenum Press, New York, 1982), vol. 27, p. 11.

4. P. A. SANGER, E. ADAM, E. IORIATTI, and S. RICHARDS, IEEE Trans. Magn. MAG-17 (1981) 666.

5. J. W. ELKIN, Cryogenics 20 611 (1980).

6. M. M. STEEVES and M. O. HOENIG, IEEE Trans. Magn. MAG-19 374 (1983).

7. H. SHIRAKI, S. MURASE, H. OHGUMA, T. HAMAJIMA, N. AOKI, and M. IOHIHARA, Cryogenics 25 13 (1983).

8. L. DRESNER, Oak Ridge National Laboratory, Oak Ridge, TN, private communication (1981).

9. J. R. MILLER and J. W. LUE, Stability of Superconductors in HeI and HeII, Proceedings of the Workshop held at Sanlay (France), (International Institute of Refrigeration, Paris, France, 1981), p. 247.

10. C. D. HENNING, B. G. LOGAN, W. L. BARR, R. H. BULMER, J. N. DOGGETT, B. M. JOHNSTON, J. D. LEE, R. W. HOARD, D. S. SLACK, and J. R. MILLER, "A Tokamak Ignition/Burn Experimental Research Device," paper 5D-2-13, this conference.

11. J. R. MILLER, J. W. LUE, R. L. BROWN, and W. J. KENNEY, IEEE Trans. Magn. MAG-17 (1981) 2250.

12. J. R. MILLER, L. DRESNER, J. W. LUE, S. S. SHEN, and H. T. YEH, in Proc. 8th Intern. Cryogenic Engineering Conference, (IPC Science and Technology Press, Ltd., Guilford, Surrey, UK, 1980), p. 321.

13. J. W. LUE, J. R. MILLER, L. DRESNER, and S. S. SHEN, in Proc. 9th Intern. Cryogenic Engineering Conference, (Butterworth & Co. (Publishers), Ltd., Guilford, Surrey, UK, 1982), p. 814.